Geodesic Paths Passing Through All Faces on A Polyhedron

Erik Demaine[1], Martin Demaine[1], David Eppstein[2], Hiro Ito[3], Yuta Katayama[3], Wataru Maruyama[3], and Yushi Uno[4]

[1] Massachusetts Institute of Technology, Cambridge, USA
{edemaine,mdemaine}@mit.edu
[2] University of California, Irvine, California, USA
eppstein@ics.uci.edu
[3] The University of Electro-Communications, Tokyo, Japan
itohiro@uec.ac.jp, uec.beryl@gmail.com
[4] Osaka Metropolitan University, Osaka, Japan
yushi.uno@omu.ac.jp

Abstract. The shortest path passing on the surface of a polyhedron is called a geodesic path. A geodesic path of a polyhedron has a property that it becomes a single line segment on a development. A geodesic path is the shortest path and it mostly passes a small number of faces. We, however, consider a problem "is there a case that a geodesic path passes all faces of a polyhedron?" For this problem the answer is "yes": we found that a regular tetrahedron has such a geodesic path. The next question is "what polyhedra have such geodesic paths?" We define a face-guard geodesic path (FGG path, for short) as a geodesic path connecting two points on a polyhedron and passing through all its faces, call a polyhedron that has an FGG path an FGG polyhedron, and try to characterize FGG polyhedra. For this new problem, we prove that there exists an FGG n-hedron for any integer $n \geq 4$, all tetrahedra and all triangular prisms with one exception are FGG polyhedra, and all cuboids and all regular polyhedra except regular tetrahedra are not FGG polyhedra.

Keywords: Geodesic paths· convex polyhedra· visability problems.

1 Introduction

The problem of the shortest distance between two points has long been discussed in various fields. The shortest path between two points on the faces of a polyhedron that passes on the faces is called a geodesic path.

Henry Dudeney presented an elemental but beautiful problem about geodesic paths, the spider and the fly [4]. There is a cuboidal room shown as Fig. 1(a), and a spider and a fly are at points p and q on the wall, respectively. What is the shortest distance the spider must crawl in order to reach the fly? This problem is to find the geodesic path between p and q. The answer is the line segment pq on a development shown in Fig. 1(b), which is a geodesic path passing through

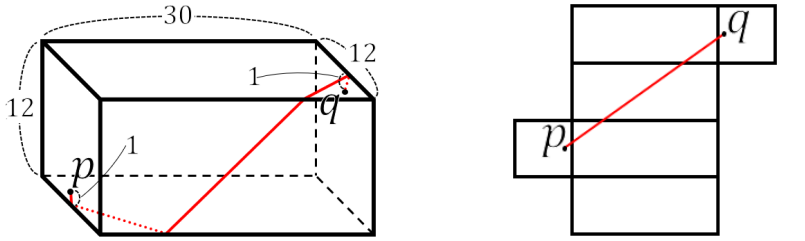

(a) A cuboid room. **(b)** A development of the cuboid.

Fig. 1: The spider and the fly.

the five faces. The question arises as to whether there is a geodesic path passing through all six faces instead of five. For this question, we proved that there is no geodesic path passing through the six faces for any cuboid. Conversely, The question naturally arises whether there is a polyhedron on which there exists a geodesic path passing through all its faces. As an answer to this question, we found that such geodesic paths exist in regular tetrahedra. We call a geodesic path that connects two points on a polyhedron and passes through all of its faces a *face-guard geodesic path*, or an *FGG path* for short, and a polyhedron that admits an FGG path is called an *FGG polyhedron*. Characterizing FGG paths and FGG polyhedra is a new and attractive problem. For this problem we obtain the following results: There exists an FGG n-hedron for any integer $n \geq 4$, all tetrahedra and all triangular prisms with one exception are FGG polyhedra, and all cuboids and all regular polyhedra except regular tetrahedra are not FGG polyhedra.

The FGG path is a new idea that was proposed by Hiro Ito and discussed at the 32nd Bellairs Winter Workshop on Computational Geometry, organized by Erik D. Demaine and Godfried Toussaint and held in Barbados in 2017. This problem, however, can be interpreted as a variation of the art gallery problem. The origin of this problem is the art gallery theorem [3] presented by Vašsek Chvátal in 1973. For an art gallery represented by a simple n-gon P, this theorem says that $\lfloor \frac{n}{3} \rfloor$ security guards with a 360° view are sufficient to guard the entire of the inside of the gallery. Based on this theorem, various visability problems have been constructed by modifying the settings of the rooms and security guards [6, 7]. The problem of guarding the faces of a polyhedron with guards replaced by lines instead of points has also been studied [2, 6]. The problem of whether FGG paths exist or not can be interpreted as a kind of visability problems for garding all faces by a geodesic paths.

The organization of this paper is as follows. In Section 2, we give preliminaries and show our results. From Sections 3 to 7, we present the proofs of these results. Concretely, Section 3 is for the proof for regular polyhedra and cuboids, Section 4 is for tetrahedra, Section 5 is for polygons and prisms, and Section 6 is for n-hedra. Finally in Section 7, we give conclusions and some conjectures.

2 Preliminaries and Results

All polyhedra treated in this paper are convex polyhedra.

2.1 Definitions

For a polyhedron and two points s and t on its faces, the shortest path passing on the face of the polyhedron between s and t is called a *geodesic path*. They are sometimes called an *s-t geodesic path* for explicitly indicating the endpoints. For a polyhedron and two points s and t on its faces, the path passing on the face of the polyhedron between the two points and which is locally the shortest is called an *s-t local geodesic path*. From the definition, the shortest path among s-t local geodesic paths is the s-t geodesic path.

A geodesic path that passes through all the faces of the polyhedron is called a *face-guard geodesic path* or an *FGG path* for short. Note that "a path passes through a face" means the path contains a part of the interior points of the face in this paper. A polyhedron that has an FGG path is called an *FGG polyhedron*.

Although this paper mainly investigates polyhedra, the idea of FGG paths is extended to 2D shapes, polygons: For a polygon, an *FGG path* is the shortest path connecting two points on the perimeter of the polygon, passing through the perimeter of the polygon, and including its interior points for every edge of the polygon. The idea of FGG paths of polygons is used for treating prisms (Theorem 4).

For a polyhedron, the maximum number of faces guarded (passed) by a geodesic path is called an *FGG number*. For a polyhedron and a pair of its two faces, the maximum number of faces guarded by a geodesic path with endpoints on the two faces is called a *face-pair FGG number*.

2.2 Basic properties

Since this research deals with convex polyhedra, the following lemma is important.

Lemma 1 ([5]). *All faces of a convex polyhedron are convex polygons.*

For geodesic paths, the following lemma holds.

Lemma 2 ([1]). *Geodesic paths do not intersect the vertices of the convex polyhedron except at endpoints.*

Since an FGG path is a kind of geodesic path, the following lemma is also obtained obviously.

Lemma 3. *An FGG path is a single line segment in a development of the convex polyhedron.*

Moreover, the following lemma holds for FGG paths.

Lemma 4. *For any convex polyhedron, an FGG path passes through any face at most once.*

Proof. It is obvious from Lemmas 1 and 2. □

Lemma 5. *For any convex polyhedron, an FGG path is not tangent to a vertex, regardless of its endpoints or internal points.*

Proof. From Lemma 2, a geodesic path does not intersect the vertices of the polyhedron except at endpoints. Assume that there exists an FGG path P with vertex v as an endpoint. Let $f_1, \ldots, f_k$ be the faces adjacent to vertex v ($k \geq 3$). From the assumption, there exists a point x_i contained in FGG path P at an interior point of f_i. The partial path between any two points on the FGG path must be an FGG path. Therefore, since the v-x_i partial path p_i of FGG path P is also an FGG path. Since f_i is convex from Lemma 1, p_i is contained in the interior points of the face f_i except v. The number of faces gathering at one vertex of a polyhedron is at least three, this FGG path must have at least three line segments emanating from v as its parts, and hence it is not a path, contradiction. □

Lemma 6. *For any convex polyhedron, The dual graph of an FGG polyhedron has a hamiltonian path.*

Proof. Obvious from Lemmas 4 and 5. □

The ultimate goal of this research is to characterize FGG polyhedra. Since this is the initial research on this topic, we mainly deal with several specific polyhedra and clarify whether or not they are FGG polyhedra. Especially for polygons, we present a necessary and sufficient conditions to have an FGG path.

2.3 Results

In this paper we present the following results.

Theorem 1. *Regular tetrahedra are FGG polyhedra. Conversely, cuboids, regular octahedra, regular dodecahedra, and regular icosahedra are not FGG polyhedra.*

Theorem 2. *For any pair of faces of any tetrahedron, the face-pair FGG number is 4. Hence every tetrahedron is an FGG polyhedron.*

Theorem 3. *A polygon has an FGG path if and only if there is a pair of adjacent edges AB and BC such that the sum of the lengths of AB and BC is larger than the sum of the lengths of the other edges.*

Theorem 4. *A prism whose base has an FGG path is an FGG polyhedron if its height is large enough.*

Theorem 5. *Triangular prisms whose base is an equilateral triangle with a side length of 1 and whose height is $\sqrt{3}$, and triangular prisms that are geometrically similar to them, are not FGG polyhedra. On the other hand, all other triangular prisms are FGG polyhedra.*

Theorem 6. *For any positive integer $n \geq 4$, there exists an FGG n-hedron.*

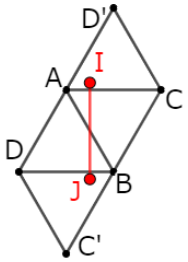

Fig. 2: A development of a regular tetrahedron and an FGG path IJ.

3 Proof of Theorem 1

In this section, we give the proof of Theorem 1. Some proofs that it is not an FGG polyhedron are obtained by the same method. The procedure is shown below.

Lemma 7. *The following procedure proves that the polyhedron P is not an FGG polyhedron.*

1. *Find $U(P)$, which is an upper bound of the length of the geodesic paths between any two points of P.*
2. *Find $L(P)$, which is a lower bound of the length of any path through all faces of P.*
3. *show $U(P) < L(P)$.*

3.1 Regular tetrahedra

First, we provide a proof that regular tetrahedra are FGG polyhedra. Later, in Theorem 2, we will show that general tetrahedra are FGG polyhedra, and thus this proof is included in the proof of Theorem 2. However, the proof of Theorem 2 is more complicated, whereas the proof for regular tetrahedra is very simple, so we provide it here separately.

Lemma 8. *Regular tetrahedra are FGG polyhedra.*

Proof. Let A, B, C, and D be the vertices of a regular tetraherdon. Consider points I and J on AC and BD, respectively, so that the line segment IJ is perpendicular to the edge AC (and DB). As shown in the development of Fig. 2, let the both ends of the line segment IJ to be slightly extended so that the both endpoints are in the interior of faces ACD' and DBC', respectively. This extended line segment is clearly an FGG path. □

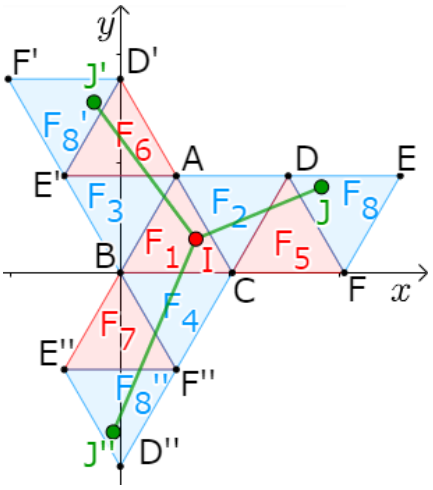

Fig. 3: An FGG path and a development of the 2-colored regular octahedron P_8 on the x-y plane.

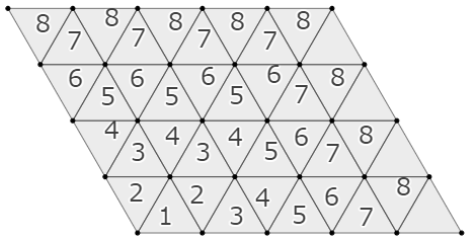

Fig. 4: The number of faces passed by a path starting from the interior of the face numbered by 1.

3.2 Regular octahedra

Lemma 9. *Regular octahedra are not FGG polyhedra.*

Proof. Consider a regular octahedron P_8 with a side length of 1. Let $U(P_8)$ be an upper bound of the length of the geodesic paths between any two points of P_8, and let $L(P_8)$ be a lower bound of the length of any path through all faces of P_8.

P_8 is 2-colorable on all its faces by coloring the adjacent faces with different colors, say red and blue. Assume that there exists an FGG path IJ on the 2-colored octahedron. Without loss of generality, I is in a red face. From Lemma 5, the path alternately passes red and blue faces and finally it ends in a blue face (see Fig. 3). Let F_1 be the red face in which I is, let F_8 be the face opposite to F_1, let F_2, F_3, and F_4 be the faces adjacent to F_1 and let F_5, F_6, and F_7 be the faces adjacent to F_8 as the development shown in Fig. 3. Let A, B, and C be the three vertices of F_1. B is placed at the origin and Side BC lies on the x-axis. Note that F_8, F_8', and F_8'' are identical. We will show $|IJ| < \sqrt{3}$ as follows.

As we discussed above, J must be in one of the blue faces. If J is in F_2, F_3, or F_4, then clearly $|IJ| < \sqrt{3}$. Thus we consider the case that J is in the interior of F_8. Let J' be a point on F_8' corresponding to J and J'' be a point on F_8'' corresponding to J (see Fig. 3). The length of the geodesic path between I and J is less than or equal to $\min\{|IJ|, |IJ'|, |IJ''|\}$ in Fig. 3. We denote vectors $\overrightarrow{BI}$

and $\overrightarrow{DJ}$ by (x_i, y_i) and (x_j, y_j), respectively. Then $\overrightarrow{IJ}, \overrightarrow{IJ'}$, and $\overrightarrow{IJ''}$ are

$$\overrightarrow{IJ} = \left(-x_i + \frac{3}{2} + x_j, -y_i + \frac{\sqrt{3}}{2} + y_j\right)$$
$$\overrightarrow{IJ'} = \left(-x_i - \frac{1}{2}x_j + \frac{\sqrt{3}}{2}y_j, -y_i + \sqrt{3} - \frac{\sqrt{3}}{2}x_j - \frac{1}{2}y_j\right)$$
$$\overrightarrow{IJ''} = \left(-x_i - \frac{1}{2}x_j - \frac{\sqrt{3}}{2}y_j, -y_i - \sqrt{3} + \frac{\sqrt{3}}{2}x_j - \frac{1}{2}y_j\right)$$

Thus, we obtain

$$\begin{aligned}
&|\overrightarrow{IJ}|^2 + |\overrightarrow{IJ'}|^2 + |\overrightarrow{IJ''}|^2 \\
=&3x_i^2 - 3x_i + 3y_i^2 - \sqrt{3}y_i + 3x_j^2 - 3x_j + 3y_j^2 + \sqrt{3}y_j + 9 \\
=&3\left\{\left(x_i - \frac{1}{2}\right)^2 + \left(y_i - \frac{1}{2\sqrt{3}}\right)^2\right\} + 3\left\{\left(x_j - \frac{1}{2}\right)^2 + \left(y_j + \frac{1}{2\sqrt{3}}\right)^2\right\} + 7 \quad (1)
\end{aligned}$$

Here $\left(x_i - \frac{1}{2}\right)^2 + \left(y_i - \frac{1}{2\sqrt{3}}\right)^2$ is the expression of a circle centered at the center of gravity of F_1 and thus $\left(x_i - \frac{1}{2}\right)^2 + \left(y_i - \frac{1}{2\sqrt{3}}\right)^2$ is maximized only when (x_i, y_i) coincides with a vertex of F_1. Considering Lemma 5, this value is less than $\frac{1}{3}$. Similarly, since $\left(x_j - \frac{1}{2}\right)^2 + \left(y_j + \frac{1}{2\sqrt{3}}\right)^2$ is the expression of a circle centered at the center of gravity of F_8 with the origin at point D and hence $\left(x_j - \frac{1}{2}\right)^2 + \left(y_j + \frac{1}{2\sqrt{3}}\right)^2 < \frac{1}{3}$. Therefore, the value of Equation (1) is smaller than 9. From this, $\min\{|IJ|, |IJ'|, |IJ''|\} < \sqrt{3}$ follows. Hence, the length of the geodesic path between I and J is less than $\sqrt{3}$, i.e., $U(P_8) = \sqrt{3}$.

Next, we estimate the lower bound on the length of the geodesic path. Observing Fig. 4, it is clear that the length of a path passing eight faces (unit regular triangles) is longer than $\sqrt{3}$, i.e., $L(P_8) > \sqrt{3}$.

From the above discussion, $U(P_8) < L(P_8)$ holds. Hence, From Lemma 7, it follows that FGG paths never exist on regular octahedra □

3.3 Regular dodecahedra

Lemma 10. *Regular dodecahedra are not FGG polyhedra.*

Proof. Consider a regular dodecahedron P_{12} with a side length of 1. Let $U(P_{12})$ be an upper bound of the length of the geodesic paths between any two points of P_{12}, and let $L(P_{12})$ be a lower bound of the length of any path through all faces of P_{12}.

The radius of the circumscribed sphere of P_{12} is $\frac{\sqrt{15}+\sqrt{3}}{4}$ [1]. Thus the maximum length of a geodesic path on the sphere is $\frac{\sqrt{15}+\sqrt{3}}{4}\pi$. For two points I and

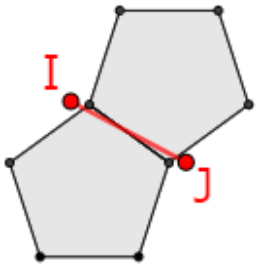

Fig. 5: A path IJ passing through two adjacent regular pentagons.

J on P_{12}, let I' and J' be points on the sphere such that I' and J' are the corresponding points of I and J, respectively, by the projection from the center of the sphere. The length of the geodesic path between I and J on P_{12} is shorter than the geodesic path between I' and J' on the sphere. Thus, $U(P_{12}) < \frac{\sqrt{15}+\sqrt{3}}{4}\pi$.

Next, we consider a path IJ passing through two regular pentagons sharing one side in the plane (see Fig. 5). Let I and J be external points of P_{12}. Clearly $|IJ| > 1$ from Fig. 5. Assume that there exists an FGG path IJ in P_{12}. We number the faces as F_1, F_2, ..., F_{12} so that path IJ passing these faces in this order. From the above discussion, for passing each adjacent pair of (F_2, F_3), (F_4, F_5), ..., (F_{10}, F_{11}) the path is required to pass distance more than one. Therefore, $L(P_{12}) > 5$ is obtained,

From the above discussion, $U(P_{12}) < L(P_{12})$ holds. Hence, From Lemma 7, FGG paths never exist on regular dodecahedra. □

3.4 Regular icosahedra

Lemma 11. *Regular icosahedra are not FGG polyhedra.*

Proof. Consider a regular icosahedron P_{20} with a side length of 1. Let $U(P_{20})$ be an upper bound of the length of the geodesic paths between any two points of P_{20}, and let $L(P_{20})$ be a lower bound of the length of any path through all faces of P_{20}.

The radius of the circumscribed sphere of the P_{20} is $\frac{\sqrt{10+2\sqrt{5}}}{4}$ [1]. By using a discussion similar to one used for regular dodecahedra, $U(P_{20}) < \frac{\sqrt{10+2\sqrt{5}}}{4}\pi$.

On the other hand, the length of a path that passes twenty faces on the P_{20} is greater than $4\sqrt{3}$ (We use an extension of Fig. 4), i.e., $L(P_{20}) > 4\sqrt{3}$.

From the above discussion, $U(P_{20}) < L(P_{20})$ holds. Hence, From Lemma 7, FGG paths never exist on regular icosahedra. □

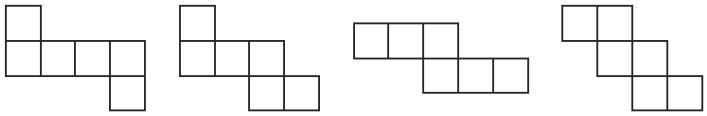

Fig. 6: The four developments in which an FGG path may exists.

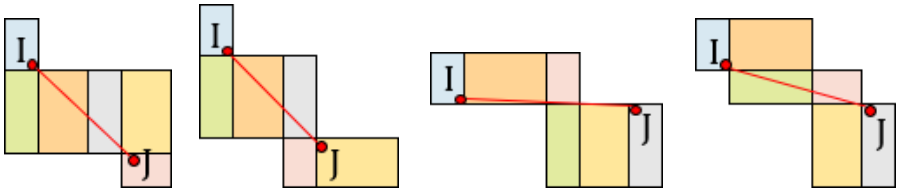

Fig. 7: The four developments of the cuboid in which an FGG path may exists.

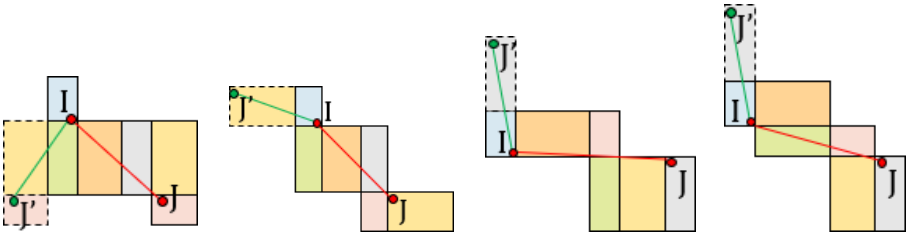

Fig. 8: Line segment IJ' shorter than IJ in each development.

3.5 Cuboids

Lemma 12. *Cuboids are not FGG polyhedra.*

Proof. First we consider a cube. Assume that there exists an FGG path on the cube. We consider a development on which the FGG path is expressed by a line segment. From Lamma 6, the dual graph of the development except for the external face must be a path. There are four such development as shown in Fig. 6.

This argument is also held for cuboids. Let a, b, and c be lengths of the sides of the cuboid. There are four possible developments of the cuboid that can construct a local geodesic path I-J passing through the six faces, as shown in Fig. 7. Note that the relative length of the edges may be changed. Without loss of generality, we can assume that the point I is located on the face of $a \times b$. For each line segment IJ in the four developments, there exists a line segment IJ' shorter than IJ (see Fig. 8), i.e., $|IJ'| < |IJ|$ holds regardless of the values of a, b, and c. From the above discussion, FGG paths never exist on cuboids. □

Now we establish the proof of Theorem 1.

Proof of Theorem 1. Obvious from Lemmas 8-12. □

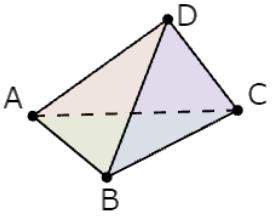

(a) A tetrahedron $ABCD$.

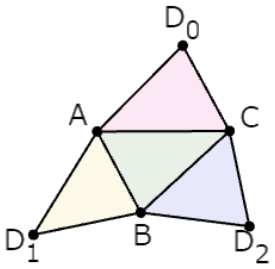

(b) A development of the tetrahedron $ABCD$.

Fig. 9: The given tetrahedron.

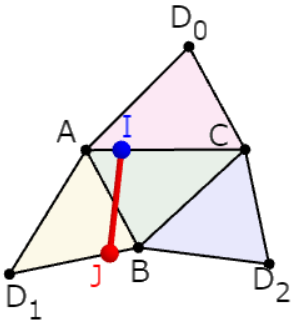

Fig. 10: A path I-J.

4 Tetrahedron

In this section, we give the proof of Theorem 2. However, this proof is complicated, and thus we will provide an outline first. First, we choose a pair of faces ABC and ABD and put points I and J on edges AC and BD, respectively, satisfying $|AI| : |IC| = |BJ| : |JD| = p : 1-p$ for a positive real number $0 < p < 1$. A path L, slightly extending both endpoints of IJ, is a path passing through the four faces. If L is a geodesic path, then L is an FGG path. Therefore, we show that there always exists a real number p, such that L becomes an FGG path, by comparing it with other paths connecting between I and J.

From here, we sometimes handle angles larger than π. To uniquely represent such angles, $\angle ABC$ denotes the angle obtained by a positive rotation from vector $\overrightarrow{BA}$ to vector $\overrightarrow{BC}$ with B at the origin and A in the positive position on the x-axis. For example, in the development in Fig. 9(b), $\angle BAC$ represents the interior angle of triangle ABC, and $\angle CAB$ represents the opposite angle.

Proof of Theorem 2. For any two faces of a given tetrahedron, let A, B, C, and D be vertices so that the two faces share edge AB (see Fig. 9). In the development of Fig. 9(a) shown in Fig. 9(b), vertices D_0, D_1, and D_2 come from the same point D in Fig. 9(a).

For a real number $0 < p < 1$, let I be a point on AC satisfying $|AI| : |IC| = p : 1-p$, and let J be a point on BD_1 satisfying $|BJ| : |JD_1| = p : 1-p$. We consider the line segment IJ (see Fig. 10). Although this path is hoped to be an I-J local geodesic path, depending on the shapes of the faces and the value of p, quadrilateral $ACBD_1$ may be non-convex and the line segment IJ may stick out from the development, which means that IJ may not be an I-J local geodesic path. To solve this problem, we prove the following lemma.

Lemma 13. *For any face pair of any tetrahedron, there exists a positive real number $p_0 > 0$ such that for every $0 < p < p_0$, IJ is an I-J local geodesic path.*

Proof. If $\angle D_1AC < \pi$ and $\angle CBD_1 < \pi$, then it is clear that the line segment IJ is an I-J local geodesic path regardless of the value of p, and thus the statement

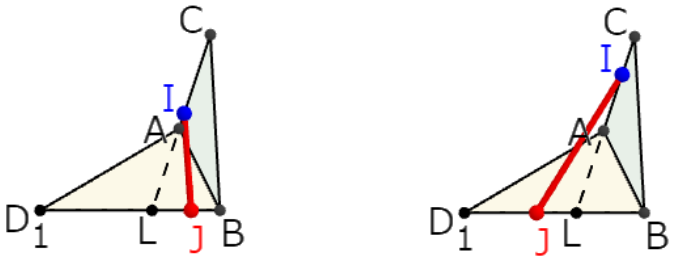

(a) $0 < p < p_0$. **(b)** $p \geq p_0$.

Fig. 11: A tetrahedron $ACBD_1$ such that $\angle D_1AC \geq \pi$.

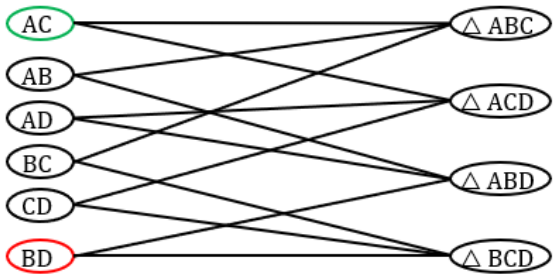

Fig. 12: Characterization of candidates of I-J local geodesic paths.

is satisfied. Therefore, in the following, we consider the case of $\angle D_1AC \geq \pi$ or $\angle CBD_1 \geq \pi$. From the symmetry, we assume the former case without loss of generality (see Fig. 11). Let L be the intersection point of lines AC and BD_1. By letting $p_0 = \frac{|BL|}{|BD_1|}$, the statement of this lemma holds. □

From Lemma 13, IJ is an I-J local geodesic path if p is small enough. Henceforth, we assume that p is small enough to satisfy the condition of Lemma 13 (thus IJ is an I-J local geodesic path). If the I-J local geodesic path in Fig. 10 is the shortest uniquely among all I-J local geodesic paths, then this I-J local geodesic path is the geodesic path and the path slightly extending both endpoints of this I-J local geodesic path is an FGG path. Therefore, we enumerate all I-J local geodesic paths and show that there always exists p such that the I-J local geodesic path in Fig. 10 is a geodesic path.

A path on a tetrahedron can be characterized by enumerating the edges and faces they passes through. For example, by traversing the I-J local geodesic path from I to J in Fig. 10, it passes edge AC, face ABC, edge AB, face ABD, and edge BD in this order. We denote it by $\langle AC, ABC, AB, ABD, BD\rangle$. This corresponds to a simple path from vertex AC to BD in the bipartite graph (see Fig. 12) such that the edge set and the face set of a tetrahedron correspond to the parts of the vertices, respectively, and an edge is assigned between vertices when the corresponding face has the corresponding edge as one of its boundaries. Thus, by enumerating the possible I-J local geodesic paths, we obtain the following

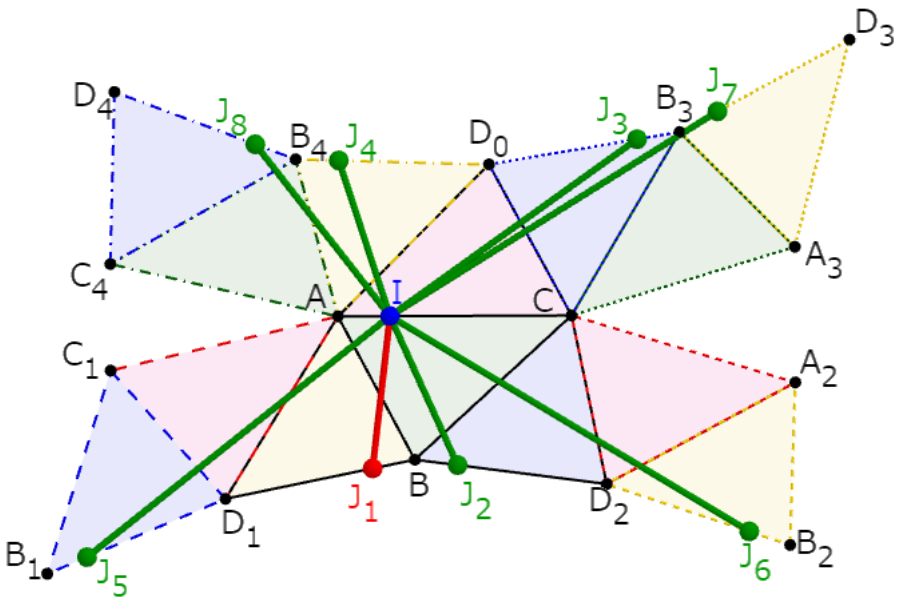

Fig. 13: Eight paths I-J_i.

8 permutations starting at the vertex AC and ending at the vertex BD in the graph of Fig. 12.

1. $\langle AC, ABC, AB, ABD, BD\rangle$
2. $\langle AC, ABC, BC, BCD, BD\rangle$
3. $\langle AC, ACD, CD, BCD, BD\rangle$
4. $\langle AC, ACD, AD, ABD, BD\rangle$
5. $\langle AC, ABC, AB, ABD, AD, ACD, CD, BCD, BD\rangle$
6. $\langle AC, ABC, BC, BCD, CD, ACD, AD, ABD, BD\rangle$
7. $\langle AC, ACD, CD, BCD, BC, ABC, AB, ABD, BD\rangle$
8. $\langle AC, ACD, AD, ABD, AB, ABC, BC, BCD, BD\rangle$

Let path I-J_i be the i-th corresponding permutation in the above enumeration. The path I-J in Fig. 10 corresponds to path I-J_1. Fig. 13 shows these eight paths I-J_i in one development. Points A, A_1, A_2 and A_3 on the development are identical in the tetrahedron. The same property holds for B, C, and D. However, depending on the shape of the tetrahedron, some of these eight line segments $IJ_1, \ldots, IJ_8$ may not be local geodesic paths. For example, if the development is as shown in Fig. 14, the path corresponding to the 2nd permutation is a polygonal line on the development (note that the path I-J_2 must cross an edge BC) and does not coincide with line segment IJ_2. In this case, there is no local geodesic path corresponding to the 2nd permutation. However, if any one of IJ_1, IJ_2, IJ_3, and IJ_4 is the shortest uniquely and is a local geodesic path, then the line segment extended at both ends very little becomes an FGG path.

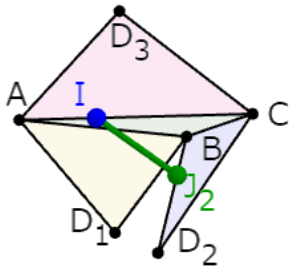

Fig. 14: A line segment IJ_2 passing outside.

Here, the existence of the local geodesic path corresponding to 1st permutation is guaranteed by Lemma 13 and it coincides with IJ_1. Therefore, regardless of the existence of local geodesic paths corresponding to the 2nd, ..., 8th permutations, we compare the lengths of line segment IJ_1 and the other line segments $IJ_2, \ldots, IJ_8$ on the development. For comparing these lengths, we consider vector as follows.

$$\begin{aligned}
\overrightarrow{IJ_1} &= \overrightarrow{IB} + \overrightarrow{BA} + \overrightarrow{AJ_1} \\
&= -\left((1-p)\overrightarrow{BA} + p\overrightarrow{BC}\right) + \overrightarrow{BA} + (1-p)\overrightarrow{AB} + p\overrightarrow{AD_1} \\
&= (1-2p)\overrightarrow{AB} + p\overrightarrow{CB} + p\overrightarrow{AD_1} \\
&= (1-2p)\overrightarrow{AB} + p\overrightarrow{CA} + p\overrightarrow{AB} + p\overrightarrow{AD_1} \\
&= (1-p)\overrightarrow{AB} + p\overrightarrow{CD_1}
\end{aligned}$$

By using similar calculations, the following equations are obtained.

$$\begin{aligned}
\overrightarrow{IJ_1} &= (1-p)\overrightarrow{AB} + p\overrightarrow{CD_1} \\
\overrightarrow{IJ_2} &= (1-p)\overrightarrow{AB} + p\overrightarrow{CD_2} \\
\overrightarrow{IJ_3} &= (1-p)\overrightarrow{AB_3} + p\overrightarrow{CD_0} \\
\overrightarrow{IJ_4} &= (1-p)\overrightarrow{AB_4} + p\overrightarrow{CD_0} \\
\overrightarrow{IJ_5} &= (1-p)\overrightarrow{AB_1} + p\overrightarrow{CD_1} \\
\overrightarrow{IJ_6} &= (1-p)\overrightarrow{AB_2} + p\overrightarrow{CD_2} \\
\overrightarrow{IJ_7} &= (1-p)\overrightarrow{AB_3} + p\overrightarrow{CD_3} \\
\overrightarrow{IJ_8} &= (1-p)\overrightarrow{AB_4} + p\overrightarrow{CD_4}
\end{aligned}$$

Next, we calculate $|\overrightarrow{IJ_i}|^2$ by using the fact $\overrightarrow{OX} \cdot \overrightarrow{OY} = \frac{|\overrightarrow{OX}|^2 + |\overrightarrow{OY}|^2 - |\overrightarrow{XY}|^2}{2}$, which is derived from the cosine formula. Note that the side length $|AB|$ is

sometimes simply expressed as AB if we have no fear of misunderstanding.

$$\begin{aligned}
|\overrightarrow{IJ_1}|^2 &= (1-p)^2AB^2 + p^2CD_1^2 + 2p(1-p)\overrightarrow{AB}\cdot\overrightarrow{CD_1} \\
&= (1-p)^2AB^2 + p^2CD_1^2 + 2p(1-p)\overrightarrow{AB}\cdot(\overrightarrow{CA}+\overrightarrow{AD_1}) \\
&= (1-p)^2AB^2 + p^2CD_1^2 - 2p(1-p)\overrightarrow{AB}\cdot\overrightarrow{AC} + 2p(1-p)\overrightarrow{AB}\cdot\overrightarrow{AD_1} \\
&= (1-p)^2AB^2 + p^2CD_1^2 - p(1-p)AB^2 - p(1-p)AC^2 + p(1-p)BC^2 \\
&+ p(1-p)AB^2 + p(1-p)AD_1^2 - p(1-p)BD_1^2 \\
&= (1-p)^2AB^2 + p(1-p)(-AC^2 + AD_1^2 + BC^2 - BD_1^2) + p^2CD_1^2
\end{aligned}$$

Similarly, we have the following equations.

$$\begin{aligned}
|\overrightarrow{IJ_1}|^2 &= (1-p)^2AB^2 + p(1-p)(-AC^2 + AD_1^2 + BC^2 - BD_1^2) + p^2CD_1^2 \\
|\overrightarrow{IJ_2}|^2 &= (1-p)^2AB^2 + p(1-p)(-AC^2 + AD_2^2 + BC^2 - BD_2^2) + p^2CD_2^2 \\
|\overrightarrow{IJ_3}|^2 &= (1-p)^2AB_3^2 + p(1-p)(-AC^2 + AD_0^2 + B_3C^2 - B_3D_0^2) + p^2CD_0^2 \\
|\overrightarrow{IJ_4}|^2 &= (1-p)^2AB_4^2 + p(1-p)(-AC^2 + AD_0^2 + B_4C^2 - B_4D_0^2) + p^2CD_0^2 \\
|\overrightarrow{IJ_5}|^2 &= (1-p)^2AB_1^2 + p(1-p)(-AC^2 + AD_1^2 + B_1C^2 - B_1D_1^2) + p^2CD_1^2 \\
|\overrightarrow{IJ_6}|^2 &= (1-p)^2AB_2^2 + p(1-p)(-AC^2 + AD_2^2 + B_2C^2 - B_2D_2^2) + p^2CD_2^2 \\
|\overrightarrow{IJ_7}|^2 &= (1-p)^2AB_3^2 + p(1-p)(-AC^2 + AD_3^2 + B_3C^2 - B_3D_3^2) + p^2CD_3^2 \\
|\overrightarrow{IJ_8}|^2 &= (1-p)^2AB_4^2 + p(1-p)(-AC^2 + AD_4^2 + B_4C^2 - B_4D_4^2) + p^2CD_4^2
\end{aligned}$$

Next, for $2 \le i \le 8$, we calculate $f_i(p) = |\overrightarrow{IJ_i}|^2 - |\overrightarrow{IJ_1}|^2$ as follows.

$$\begin{aligned}
f_2(p) =& |\overrightarrow{IJ_2}|^2 - |\overrightarrow{IJ_1}|^2 \\
=& (1-p)^2AB^2 + p(1-p)(-AC^2 + AD_2^2 + BC^2 - BD_2^2) + p^2CD_2^2 \\
& - \left\{(1-p)^2AB^2 + p(1-p)(-AC^2 + AD_1^2 + BC^2 - BD_1^2) + p^2CD_1^2\right\} \\
=& p(1-p)(AD_2^2 - AD_1^2) + p^2(CD_2^2 - CD_1^2) \\
=& p^2(AD_1^2 - AD_2^2 + CD_2^2 - CD_1^2) + p(AD_2^2 - AD_1^2)
\end{aligned}$$

Similarly, we have the following equations.

$$\begin{aligned}
f_2(p) =& p^2(AD_1^2 - AD_2^2 + CD_2^2 - CD_1^2) + p(AD_2^2 - AD_1^2) \\
f_3(p) =& p^2(AB_3^2 - AB^2 + CD_0^2 - CD_1^2) + p(2AB^2 - 2AB_3^2) + AB_3^2 - AB^2 \\
f_4(p) =& p^2(BC^2 - B_4C^2 + CD_0^2 - CD_1^2) + p(B_4C^2 - BC^2) \\
f_5(p) =& p^2(AB_1^2 - AB^2 + BC^2 - B_1C^2) \\
& + p(2AB^2 - 2AB_1^2 + B_1C^2 - BC^2) + AB_1^2 - AB^2
\end{aligned}$$

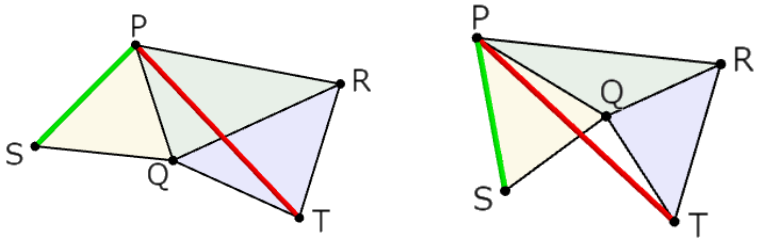

(a) $\angle TQP \leq \pi$. **(b)** $\angle TQP > \pi$.

Fig. 15: A pentagon $SPRTQ$ consisting of three faces of a tetrahedron.

$$\begin{aligned}
f_6(p) =& p^2(AB_2^2 - AB^2 + AD_1^2 - AD_2^2 + BC^2 - B_2C^2 + CD_2^2 - CD_1^2) \\
&+ p(AD_2^2 - AD_1^2 + B_2C^2 - BC^2 + 2AB^2 - 2AB_2^2) + AB_2^2 - AB^2 \\
f_7(p) =& p^2(AB_3^2 - AB^2 + AD_1^2 - AD_3^2) \\
&+ p(AD_3^2 - AD_1^2 - 2AB^2 - 2AB_3^2) + AB_3^2 - AB^2 \\
f_8(p) =& p^2(AD_1^2 - AD_4^2 + BC^2 - B_4C^2 + CD_4^2 - CD_1^2) \\
&+ p(AD_4^2 - AD_1^2 + B_4C^2 - BC^2)
\end{aligned}$$

We show that there exists $p > 0$ in a neighborhood of $p = 0$ where all these seven equations $f_i(p)$ are positive. To investigate the properties of these equations in the neighborhood of $p = 0$, we calculate the limit of $p \to 0$.

$$\begin{aligned}
&\lim_{p\to 0} f_2(p) = 0, && \lim_{p\to 0} f_3(p) = AB_3^2 - AB^2, && \lim_{p\to 0} f_4(p) = 0, \\
&\lim_{p\to 0} f_5(p) = AB_1^2 - AB^2, && \lim_{p\to 0} f_6(p) = AB_2^2 - AB^2, && \lim_{p\to 0} f_7(p) = AB_3^2 - AB^2, \\
&\lim_{p\to 0} f_8(p) = 0.
\end{aligned}$$

We consider these seven equations in three parts: $\{f_3, f_5, f_7\}, \{f_2, f_4, f_8\}$, and $\{f_6\}$ and consider them one by one. In preparation for these discussions, we present the following lemma.

Lemma 14. *For any three distinct faces of any tetrahedron, we consider a development shown as Fig. 15 (the symbols are assigned arbitrarily). Then, $PS < PT$.*

Proof. Since it is a development of a tetrahedron, $|QS| = |QT|$. From the facts that $\angle PQS < \angle TQP$ if $\angle TQP \leq \pi$ and $\angle PQS < \angle PQT$ if $\angle TQP > \pi$, the statement of this lemma follows. □

First, we consider f_3, f_5, and f_7. By applying Lemma 14 to faces ABD_1, AC_1D_1, and $B_1C_1D_1$, $AB_1 > AB$ holds. Similarly, $AB_3 > AB$ also holds. Therefore, $\lim_{p\to 0} f_3(p) > 0, \lim_{p\to 0} f_5(p) > 0$, and $\lim_{p\to 0} f_7(p) > 0$ hold. Hence, f_3, f_5, and f_7 are positive if $p > 0$ is small enough.

Next, we consider f_2, f_4, and f_8. Since $\lim_{p\to 0} f_2(p) = 0, \lim_{p\to 0} f_4(p) = 0$, and $\lim_{p\to 0} f_8(p) = 0$, if $\lim_{p\to 0} f_2'(p), \lim_{p\to 0} f_4'(p)$, and $\lim_{p\to 0} f_8'(p)$ are positive, then f_2, f_4, and f_8 are positive in a neighborhood of $p = 0$. By differentiating

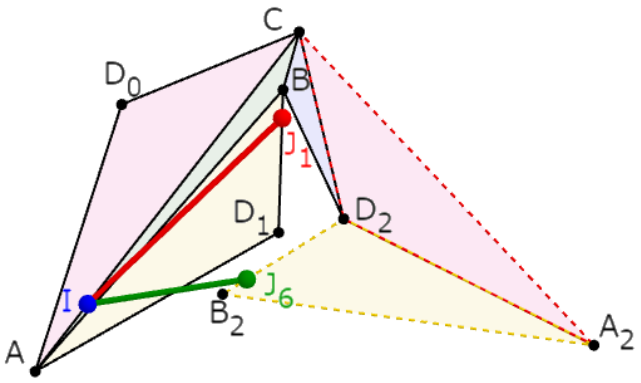

Fig. 16: A case of $f_6 < 0$ if $p > 0$ is infinitedecimally close to 0.

f_2, f_4, and f_8, and taking the limit of $p = 0$ for the differential coefficients, we obtain

$$\lim_{p\to 0} f_2'(0) = AD_2^2 - AD_1^2, \qquad \lim_{p\to 0} f_4'(0) = B_4C^2 - BC^2,$$
$$\lim_{p\to 0} f_8'(0) = AD_4^2 - AD_1^2 + B_4C^2 - BC^2.$$

By using Lemma 14 for faces ABD_1, AC_1D_1 and $B_1C_1D_1$, $AD_2 > AD_1$ holds. Similarly, $B_4C > BC$ also holds. From $AD_2 = AD_4$, $AD_4 > AD_1$ also holds. Therefore, since $AB_1 > AB$ was shown in the proof for f_3, f_5, and f_7, $\lim_{p\to 0} f_2'(p) > 0, \lim_{p\to 0} f_4'(p) > 0$, and $\lim_{p\to 0} f_8'(p) > 0$ hold. Hence, f_2, f_4, and f_8 are positive if $p > 0$ is small enough.

Finally, we consider f_6. For f_6, there exists a case where $f_6 < 0$, i.e. $IJ_6 < IJ_1$ even if $p > 0$ is infinitedecimally close to 0 (see Fig. 16). Therefore, we cannot use the strategy of showing $f_6 > 0$ regardless of the existence of local geodesic paths. Thus, for f_6, we show that $\lim_{p\to 0} f_6(p) > 0$ if the path I-J_6 is a local geodesic path in the neighborhood of $p = 0$. Since $\lim_{p\to 0} f_6(p) = AB_2^2 - AB^2$, we show $AB_2 > AB$ under the assumption that the path I-J_6 is a local geodesic path in the neighborhood of $p = 0$. If line segment AB_2 is not a local geodesic path, then the path I-J_6 is also not a local geodesic path by taking p close enough to 0. Thus, in the following, we consider the case where the line segment AB_2 is a local geodesic path (see Fig. 17). Under this assumption, the following observations are obtained.

Observation 7 *A line segment AB_2 passes through faces ABC,BCD_2,A_2CD_2, and $A_2B_2D_2$ in this order and intersects with line segments BC,CD_2, and A_2D_2.*

From this observation, the following lemma holds.

Lemma 15. *$\angle AB_2D_2 \leq \angle A_2B_2D_2$ and $\angle BAB_2 \leq \angle BAC$.*

Proof. Obvious from observation 7. □

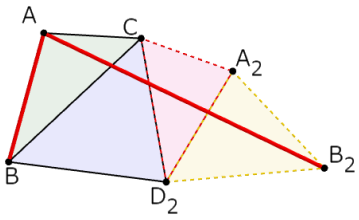

Fig. 17: AB and AB_2.

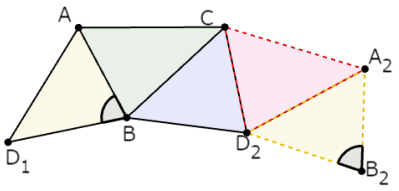

Fig. 18: $\angle A_2B_2D_2$ and $\angle ABD_2$.

Lemma 16. $\angle A_2B_2D_2 < \angle D_2BA$.

Proof. In the development shown in Fig. 18, $\angle ABD_1$, and $\angle A_2B_2D_2$ are identical. By considering similarly to the proof of Lemma 14, $\angle ABD_1 < \angle D_2BA$. Hence, $\angle A_2B_2D_2 = \angle ABD_1 < \angle D_2BA$. □

We will consider each possible cases of $\angle BAB_2$ in turn.

Case 1 ($0 < \angle BAB_2 < \pi$)
From Lemmas 15 and 16, we obtain $\angle AB_2D_2 < \angle D_2BA$. Since D_2BB_2 is an isosceles triangle, $\angle BB_2D_2 = \angle D_2BB_2$. Here, if $\angle ABB_2 \leq \angle ABD_2$ (see Fig. 19(a)), then $\angle AB_2D_2 = \angle AB_2B + \angle D_2B_2B$ and $\angle D_2BA = \angle B_2BA + \angle B_2BD_2$. Also, if $\angle ABB_2 > \angle ABD_2$ (see Fig. 19(b)), then $\angle AB_2D_2 = \angle AB_2B - \angle D_2B_2B$ and $\angle D_2BA = \angle B_2BA - \angle B_2BD_2$. Hence, we obtain $\angle AB_2B < \angle B_2AB$ and hence from the size relationship between sides and angles $AB < AB_2$ follows.

Case 2 (A, B, **and** B_2 **are colinear**)
There are three cases: $\langle A, B, B_2\rangle$, $\langle A, B_2, B\rangle$, and $\langle B, A, B_2\rangle$. In the case of $\langle A, B, B_2\rangle$, $AB < AB_2$ obviously holds (see Fig.20). In the case of $\langle A, B_2, B\rangle$, B_2 never be on edge AB and hence this order does not exist. In the case of $\langle B, A, B_2\rangle$, $\angle BAB_2 = \pi$. From that $\angle BAC$ is an inner angle of a triangle, $\angle BAC < \pi$ follows, and thus $\angle BAC < \angle BAB_2$. On the other hand, from Lemma 15, $\angle BAB_2 \leq \angle BAC$ follows, contradiction.

Case 3 ($\pi < \angle BAB_2 < 2\pi$)
In this case, AB_2 is not a local geodesic path because AB_2 passes outside of the development (see Fig.21).

The results of these three case divisions indicate that if the path I-J_6 are local geodesics, then $AB < AB_2$. Hence, if path I-J_6 is a local geodesic path, then f_6 is positive if $p > 0$ is small enough.

From the above discussion, we have shown that IJ_1 is the uniquely shortest local geodesic path among $IJ_1, \ldots, IJ_8$ if $p > 0$ is small enough. Therefore, a line segment obtained by slightly extending the both ends of IJ_1 is the desired FGG path. Here, because of the arbitrariness of the choice of faces at the endpoints of the IJ at the beginning of this proof, any tetrahedron is an FGG polyhedron and the face-pair FGG number is 4.

□

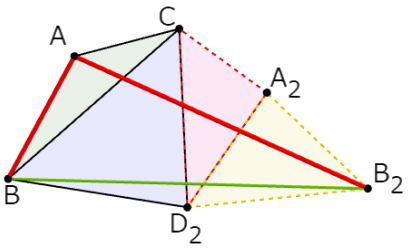

(a) $\angle ABB_2 \leq \angle ABD_2$.

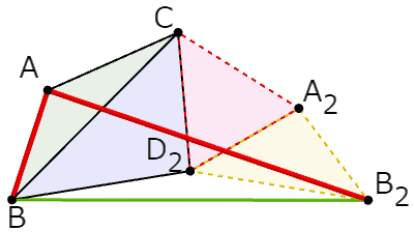

(b) $\angle ABB_2 > \angle ABD_2$.

Fig. 19: Case 1 ($0 < \angle BAB_2 < \pi$).

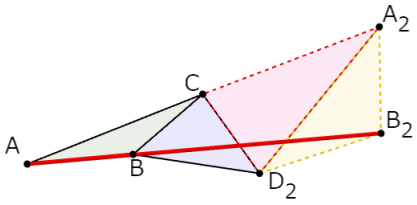

Fig. 20: Case 2 (A, B, and B_2 are colinear).

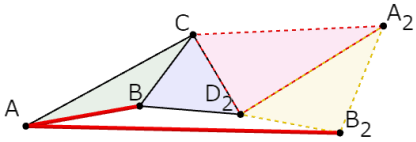

Fig. 21: Case 3 ($\pi < \angle BAB_2 < 2\pi$).

5 Polygons and Prisms

5.1 Polygons

The properties of an FGG path on a prism should closely depend on the shape of its base (and ceiling). Therefore, we first show the properties of FGG paths on polygons and discuss the properties of prisms afterward. We obtain a necessary and sufficient condition of a polygon to have an FGG path as follows.

Theorem 3. *A polygon has an FGG path if and only if there is a pair of adjacent edges AB and BC such that the sum of the lengths of AB and BC is larger than the sum of the lengths of the other edges (see Fig.22).*

Proof. Take a point p on edge AB and a point q on edge BC to satisfy $|Ap| = |Cq| = \epsilon > 0$. If ϵ is small enough, the p-q geodesic path is clearly an FGG path.

Next, for an n-gon ($n \geq 3$), we assume that there is no such a pair of adjacent edges. Let ℓ be the sum of the length of all edges. For any point p on the perimeter of the polygon, let $o(p)$ be the opposite point on the perimeter, i.e., the length of the two (turning clockwise or counterclockwise) p-$o(p)$ geodesic paths (i.e., passing through edges) are both $\ell/2$. From the assumption, for any p-$o(p)$ geodesic path, there is an edge that is not included in the path. Thus, these paths are not FGG paths. □

(a) A triangle ABC. **(b)** A hexagon $ABCDEF$.

Fig. 22: Polygons that have FGG paths.

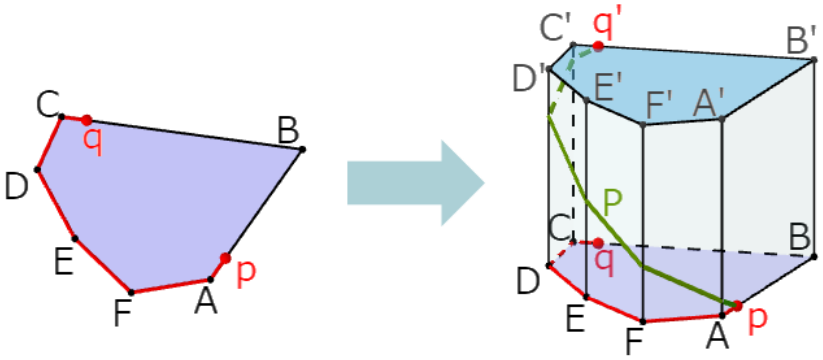

Fig. 23: Constructing a prism from a polygon that has an FGG path.

5.2 Prisms whose bases are FGG polygons

Next, we discuss prisms.

Theorem 4. *A prism whose base has an FGG path is an FGG polyhedron if it's hight is large enough.*

Proof. Let p and q be the endpoints of the FGG path of the base polygon. We use the symbols used in Theorem 3, and hence p and q are interior points of AB and BC, respectively. Let q' be the point of the ceiling corresponding to q (see Fig. 23). A local geodesic path p-q' shown in the right figure of Fig. 23, which is denoted by P, passes all side faces. Hence, a path obtained by slightly extending both endpoints of P so that the endpoints are in the ceiling and the base, respectively, passes all faces. Thus, we prove that P is the uniquely shortest local geodesic path.

For this purpose, we compare P with other p-q' local geodesic paths. Any p-q' local geodesic paths can be characterized as follows: after starting from p, it passes on the base, on the side faces, and finally on the ceiling (see Fig. 24). We denote the length of the part of the base, the side faces, and the ceiling of the path by l_1, l_2, and l_3, respectively. The lengths of these paths are expressed as $l_1 + l_2 + l_3$. Note that for P, $l_1 + l_3 = 0$. Furthermore, let s be the length of

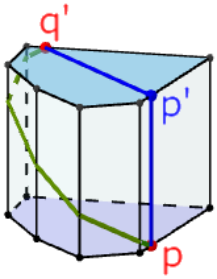

(a) Path P'.

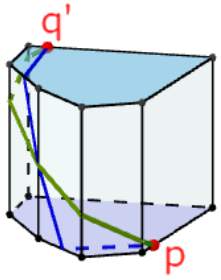

(b) Path P''.

Fig. 24: Examples of other p-q' local geodesic paths.

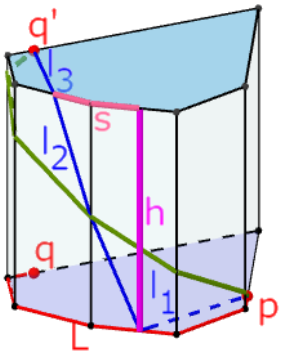

Fig. 25: Illustration of s, L.

the projection of l_2 onto the base, and hence $l_1 + l_2 + l_3 = l_1 + \sqrt{h^2 + s^2} + l_3$ where h is the hight of the prism (see Fig. 25). Let L be the length of the FGG path between pq on the base, and hence the length of P can be expressed as $\sqrt{h^2 + L^2}$. Furthermore, we denote $l_1 + l_3$ as l_{1+3} for simplicity.

We show that there exists real number $h_0 > 0$ such that the following inequality holds.

$$\sqrt{h^2 + L^2} < l_{1+3} + \sqrt{h^2 + s^2} \tag{2}$$

Note that we only need to consider the case where $l_{1+3} > 0$, i.e., $0 \leq s < L$. Also, obviously $h > 0$ and $L > 0$. Furthermore, since the base is a convex polygon, $0 \leq l_1 < L$, $0 \leq l_3 < L$, and $l_{1+3} + s < L$ hold. By using these inequalities, the following inequality can be derived from Inequality (2).

$$\begin{aligned}
\sqrt{h^2 + L^2} &< l_{1+3} + \sqrt{h^2 + s^2} \\
h^2 + L^2 &< l_{1+3}^2 + 2l_{1+3}\sqrt{h^2 + s^2} + h^2 + s^2 \\
\sqrt{h^2 + s^2} &> \frac{L^2 - s^2 - l_{1+3}^2}{2l_{1+3}}
\end{aligned}$$

Since $L > s + l_{1+3}$, we can square both sides.

$$\begin{aligned}
h^2 + s^2 &> \frac{(L^2 - s^2 - l_{1+3}^2)^2}{4l_{1+3}^2} \\
h^2 &> \frac{(L^2 - s^2 - l_{1+3}^2)^2 - 4s^2 l_{1+3}^2}{4l_{1+3}^2} \\
h^2 &> \frac{(L^2 - s^2 - l_{1+3}^2 + 2sl_{1+3})(L^2 - s^2 - l_{1+3}^2 - 2sl_{1+3})}{4l_{1+3}^2} \\
h^2 &> \frac{(L^2 - (s + l_{1+3})^2)(L^2 - (s - l_{1+3})^2)}{4l_{1+3}^2}
\end{aligned}$$

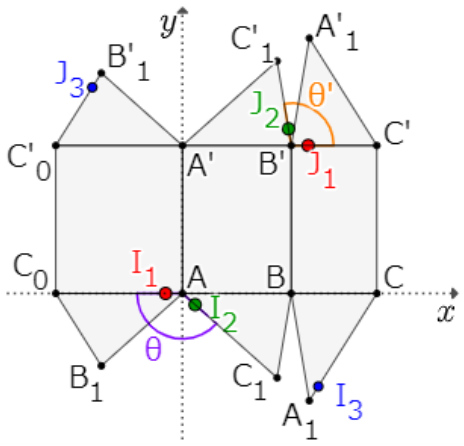

Fig. 26: A development of a triangular prism on the coordinate plane.

Since $h > 0$, $L > s + l_{1+3}$, $L^2 > (s - l_{1+3})^2$, and $l_{1+3} > 0$, we can take the square root of both sides.

$$h > \sqrt{\frac{(L^2 - (s + l_{1+3})^2)(L^2 - (s - l_{1+3})^2)}{4l_{1+3}^2}}$$

$$h > \frac{\sqrt{(L + s + l_{1+3})(L - s - l_{1+3})(L + s - l_{1+3})(L - s + l_{1+3})}}{2l_{1+3}}$$

Since the value of the right side is finite, it is the desired value of h_0. □

5.3 Triangular prisms

Triangles have FGG paths. Therefore, a triangular prism with enough height is an FGG polyhedron from Theorem 4. However, we present a complete characterization of FGG triangular prisms as follows.

Theorem 5. *A triangular prism whose base is an equilateral triangle with a side length of 1 and whose height is $\sqrt{3}$, and triangular prisms that are geometrically similar to them, are not FGG polyhedra. On the other hand, all other triangular prisms are FGG polyhedra.*

Proof. Consider a development of a triangular prism whose base and ceiling are ABC and $A'B'C'$, respectively, drawn on the coordinate plane (see Fig. 26). The origin is A, and the side edges adjacent to the base are placed on the x-axis. Let $|AB| = 1$ for a normalization and let h be the height of the triangular prism. The subscripted points C, C_0, and C_1 are the identical points in the triangular prism. The same holds for A, B, A', B', and C'. For real numbers p and q, let I be a point on edge AC such that $|AI| = p$, and J be a point on edge BC such that $|BJ| = q$. I and J are indicated as I_1, I_2, I_3, and J_1, J_2, J_3

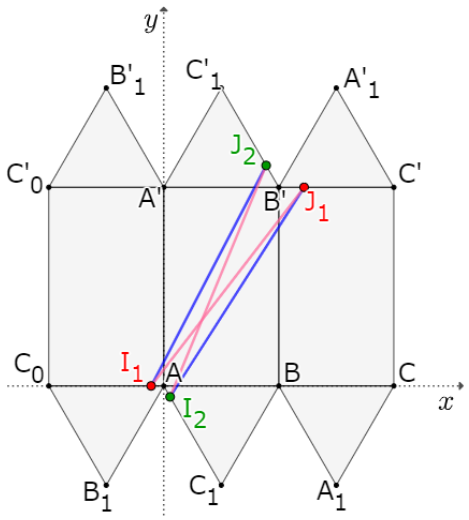

Fig. 27: The equilateral triangular prisms with $|AB| = 1$ and $|AA'| = \sqrt{3}$.

on the development, respectively. Candidates of the I-J geodesic path are line segments I_iJ_j $(i, j \in \{1, 2, 3\})$. From $|AB'| < |AB'_1|$ and $|AB'| < |A_1B'|$, I_3J_j and I_iJ_3 $(i, j \in \{1, 2, 3\})$ can not be the shortest if p and q are both tiny values. Line segments I_1J_1, I_1J_2, I_2J_1, and I_2J_2 do not pass through the outside of the development if p and q are small enough. Hence, if any one of these paths is uniquely the shortest, then a path slightly extending both endpoints of the shortest one is an FGG path. Let $\theta = \angle C_0AC_1$ and $\theta' = \angle C'B'C'_1$. Then, points I_1, I_2, J_1, and J_2 are denoted by $I_1 = (-p, 0), I_2 = (-p\cos\theta, -p\sin\theta), J_1 = (1 + q, h)$, and $J_2 = (1 + q\cos\theta', h + q\sin\theta')$. By using them, we obtain

$$
\begin{aligned}
|I_1J_1|^2 &= p^2+q^2+h^2+1+2(p + q + pq),\\
|I_1J_2|^2 &= p^2+q^2+h^2+1+2(p + q(\cos\theta' + h\sin\theta') + pq\cos\theta'),\\
|I_2J_1|^2 &= p^2+q^2+h^2+1+2(p(\cos\theta + h\sin\theta) + q + pq\cos\theta),\\
|I_2J_2|^2 &= p^2+q^2+h^2+1+2\left(p(\cos\theta+h\sin\theta)+q(\cos\theta'+h\sin\theta')+pq\cos(\theta-\theta')\right).
\end{aligned}
$$

Observing these equations, if $\theta = \theta'$ and $\cos\theta + h\sin\theta = 1$, then $|I_1J_2| = |I_2J_1|$ and $|I_1J_1| = |I_2J_2|$, regardless of the value of p and q. Conversely, if $\theta \neq \theta'$ or $\cos\theta + h\sin\theta \neq 1$, then we can make one of $|I_1J_1|$, $|I_1J_2|$, $|I_2J_1|$, and $|I_2J_2|$ be uniquely the shortest by adjusting the value of p and q (even if p and q are very small). Since there is a freedom to assign vertices to be A and B, the unique case where $\theta = \theta'$ is always true is the case where the base is an equilateral triangle, i.e. $\theta = \theta' = \frac{2}{3}\pi$. In this case, from $\cos\theta + h\sin\theta = 1$, we obtain $h = \sqrt{3}$. This is the triangular prisms whose base is an equilateral triangle with a side length of 1 and whose height is $\sqrt{3}$ (see Fig. 27). Therefore, we showed that except triangular prism geometrically similar to this, all triangular prisms are FGG polyhedra.

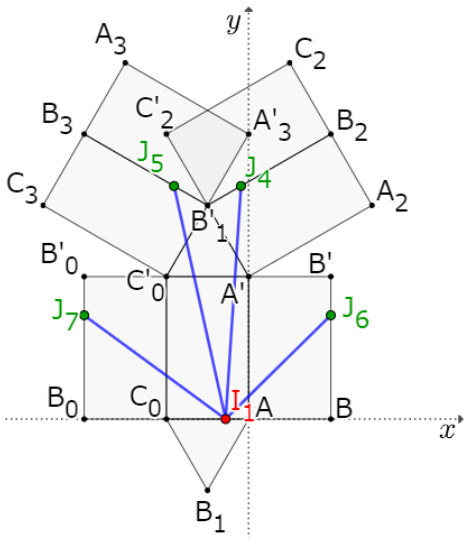

Fig. 28: Four candidates for point J.

Finally, we show that equilateral triangular prisms with base length 1 and height $\sqrt{3}$ and similar equilateral triangular prisms are not FGG polyhedra. Assume that equilateral triangular prisms with base length 1 and height $\sqrt{3}$ have an FGG path. From the symmetry, we only need to consider the following four orders of the faces through which the FGG path passes.

Case 1 ⟨base, side, side, side, ceiling⟩
Case 2 ⟨base, side, side, ceiling, side⟩
Case 3 ⟨base, side, ceiling, side, side⟩
Case 4 ⟨side, base, side, ceiling, side⟩

From the symmetry, assume that AC is the base edge traversed by the FGG path. Case 1 corresponds to the line segment I_1J_1, Case 2 corresponds to the line segments I_1J_2 and J_1I_2, Case 4 corresponds to the line segment I_2J_2 in Fig. 27, respectively, and they are not FGG paths since $|I_1J_2| = |I_2J_1|$ and $|I_1J_1| = |I_2J_2|$. Finally, we discuss the case 3. A path passing through in this order obtained from the line segments I_1J_4 or I_1J_5 shown in Fig. 28 by extending both endpoints. In this case, there exist two other candidates, I_1J_6 and I_1J_7, for the FGG path as shown Fig. 28 . We compare the lengths of them. Let $|AI| = p$ and $|BJ| = q$. From the symmetry, we can assume that $p \leq \frac{1}{2}$ without loss of generality, and hence, only IJ_4 and IJ_6 are candidates. The coordinates of each point are $I_1 = (-p, 0), J_4 = \left(\frac{\sqrt{3}}{2}q - \frac{1}{2}, \frac{1}{2}q + \frac{3\sqrt{3}}{2}\right)$, and $J_6 = \left(1, \sqrt{3} - q\right)$. Hence, we obtain $|I_1J_4|^2 = p^2 + \sqrt{3}pq - p + q^2 + \sqrt{3}q + 7$ and $|I_1J_6|^2 = p^2 + 2p + qq^2 - 2\sqrt{3}q + 4$. From the assumption that this equilateral triangular prism has an FGG path of case 3, the following must hold.

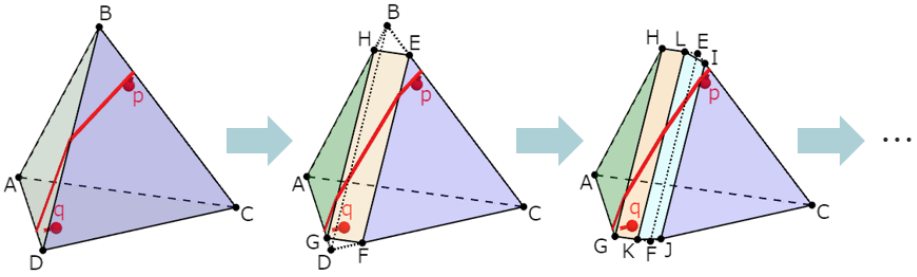

Fig. 29: An example of inductively increasing the number of faces by chamfering.

$$|I_1J_4|^2 - |I_1J_6|^2 = \sqrt{3}pq - 3p + 3\sqrt{3}q + 3 < 0. \tag{3}$$

Since $0 < p \leq \frac{1}{2}, 0 < q < \sqrt{3}$, we obtain

$$q < \frac{\sqrt{3}(p-1)}{p+3}. \tag{4}$$

The right side of Inequality (4) is always less than 0, contradiction. □

6 *n*-hedra

In this section, we give the proof of Theorem 6.

Proof of Theorem 6. For $n = 4$, tetrahedra have FGG paths (Theorem 2) and the statement holds. Next, we assume that there exists an FGG n-hedron. Let e be one of the edges of the n-hedron that is crossed by an FGG path. We now cut e off very thinly by a plane parallel to the edge e (see Fig. 29). This operation is called *chamfering*. A chamfering make an n-hedron to be an $n+1$-hedron. Moreover, since the thickness of the chamfering can be made as small as possible, the new polyhedron is also an FGG polyhedron. By induction, the statement of this theorem is proven.

□

7 Conclusions and Conjectures

In this paper, we proposed the concepts of FGG polyhedra, FGG numbers, and face-pair FGG numbers, and clarified whether a polyhedron is an FGG polyhedron or not for several polyhedra. Our primary goal of this study is to characterize FGG polyhedra, i.e., to classify all polyhedra as FGG polyhedra or not. Furthermore, there is also the goal of clarifying the FGG numbers and face-pair FGG numbers of polyhedra. To achieve these goals, we will work on proving whether a polyhedron is an FGG polyhedron or not for more other polyhedra. As immediate goals, we have the following conjectures.

Conjecture 1 *Bipyramids are not FGG polyhedra.*

Conjecture 2 *Truncated regular polyhedra and chamfered regular polyhedra are not FGG polyhedra.*

For polygons, we conjecture that the condition of Theorem 4 is a necessary and sufficient condition, i.e., we also have the following conjecture.

Conjecture 3 *A necessary and sufficient condition for a polygon P to have an FGG path is that a prism with enough height having P as its base is an FGG polyhedron.*

Acknowledgements

The authors would like to express their deep appreciation to the participants of the 32nd Bellairs Winter Workshop on Computational Geometry, 2017, for their fruitful discussions. We also thank the anonymous referees for their valuable comments, which improved this papers. Hiro Ito is supported by JSPS KAKENHI 15K11985 and 20K11671.

References

1. Alexandrov, A.D.: Convex polyhedra, vol. 109. Springer (2005)
2. Bose, P., Shermer, T., Toussaint, G., Zhu, B.: Guarding polyhedral terrains. Computational Geometry **7**(3), 173–185 (1997)
3. Chvátal, V.: A combinatorial theorem in plane geometry. Journal of Combinatorial Theory, Series B **18**(1), 39–41 (1975)
4. Dudeney, H.E.: The Canterbury Puzzles. Courier Corporation (2002)
5. Matousek, J.: Lectures on discrete geometry, vol. 212. Springer Science & Business Media (2013)
6. O'rourke, J.: Art gallery theorems and algorithms. Oxford University Press (1987)
7. Shermer, T.C.: Recent results in art galleries (geometry). Proceedings of the IEEE **80**(9), 1384–1399 (1992)